Exchange of associated factors directs a switch in HBO1 acetyltransferase histone tail specificity

Marie-Eve Lalonde,[1] Nikita Avvakumov,[1] Karen C. Glass,[2,7] France-Hélène Joncas,[1] Nehmé Saksouk,[1] Michael Holliday,[3] Eric Paquet,[1] Kezhi Yan,[5] Qiong Tong,[2] Brianna J. Klein,[2] Song Tan,[4] Xiang-Jiao Yang,[5,6] Tatiana G. Kutateladze,[2,3] and Jacques Côté[1,8]

[1]Laval University Cancer Research Center, Hôtel-Dieu de Québec (CHUQ), Quebec City, Québec G1R 2J6, Canada; [2]Department of Pharmacology, [3]Molecular Biology Program, University of Colorado School of Medicine, Aurora, Colorado 80045, USA; [4]Center for Gene Regulation, Department of Biochemistry and Molecular Biology, The Pennsylvania University, University Park, Pennsylvania 16802, USA; [5]The Rosalind and Morris Goodman Cancer Research Center, Department of Biochemistry, McGill University, Montreal, Québec H3A 1A1, Canada; [6]Department of Medicine, McGill University Health Center, Montreal, Québec H3A 1A1, Canada

Histone acetyltransferases (HATs) assemble into multisubunit complexes in order to target distinct lysine residues on nucleosomal histones. Here, we characterize native HAT complexes assembled by the BRPF family of scaffold proteins. Their plant homeodomain (PHD)–Zn knuckle–PHD domain is essential for binding chromatin and is restricted to unmethylated H3K4, a specificity that is reversed by the associated ING subunit. Native BRPF1 complexes can contain either MOZ/MORF or HBO1 as catalytic acetyltransferase subunit. Interestingly, while the previously reported HBO1 complexes containing JADE scaffold proteins target histone H4, the HBO1–BRPF1 complex acetylates only H3 in chromatin. We mapped a small region to the N terminus of scaffold proteins responsible for histone tail selection on chromatin. Thus, alternate choice of subunits associated with HBO1 can switch its specificity between H4 and H3 tails. These results uncover a crucial new role for associated proteins within HAT complexes, previously thought to be intrinsic to the catalytic subunit.

[*Keywords*: acetyltransferase complexes; PHD fingers; histone tails; MYST family; chromatin acetylation; BRPF1]

Supplemental material is available for this article.

Received May 29, 2013; revised version accepted August 23, 2013.

In eukaryotic cells, DNA wraps around histone octamers to form nucleosomes, the basic units of chromatin. This structural organization not only allows compaction of the DNA in the nuclei, but also regulates diverse cellular processes such as DNA repair, transcription, and replication. This regulation is mainly exerted via the different post-translational modifications of the protruding N-terminal tail residues of histones, such as acetylation, methylation, phosphorylation, ubiquitination, and sumoylation. These modifications act as docking sites for different protein effectors involved in many cell pathways (Musselman et al. 2012). Acetylation of histone lysines is one of the best-characterized functional modifications. It is deposited by histone acetyltransferases (HATs) by transferring the acetyl group from acetyl-CoA on the ε-amino group of lysine residues. Although histone acetylation has mostly been associated with transcriptional activators and regulators, it has also been implicated in other processes, such as DNA repair and replication and mRNA splicing (Shahbazian and Grunstein 2007; van Attikum and Gasser 2009; de Almeida and Carmo-Fonseca 2012).

The MYST (MOZ, Ybf2/Sas3, Sas2, and Tip60) family of acetyltransferases is composed of evolutionarily conserved enzymes that are assembled into multisubunit protein complexes. They acetylate histone tails within chromatin but also target nonhistone substrates in both humans and yeast (Sapountzi and Cote 2011). We previously purified several native MYST complexes and found that they are based on a tetrameric core structure associated with an ING tumor suppressor subunit, the Eaf6 subunit, and an EPC (enhancer of polycomb)-related scaffold subunit (Doyon et al. 2006; Saksouk et al. 2009; Avvakumov et al. 2012). Four human MYST complexes assemble in such a manner; namely, Tip60 (KAT5), HBO1 (MYST2 and KAT7), MOZ (MYST3 and KAT6A), and

[7]**Present address: Department of Pharmaceutical Sciences, Albany College of Pharmacy and Health Sciences, Colchester, VT 05446, USA.**
[8]**Corresponding author**
E-mail jacques.cote@crhdq.ulaval.ca
Article is online at http://www.genesdev.org/cgi/doi/10.1101/gad.223396.113.

MORF (MYST4 and KAT6B) (Fig. 1A). These enzymes have been shown to play crucial roles in DNA repair, recombination, and replication as well as in transcription activation (Avvakumov and Cote 2007b), which in turn regulates developmental processes (Voss and Thomas 2009) and is involved in leukemia and several genetic diseases (Avvakumov and Cote 2007a; Yang and Ullah 2007; Voss and Thomas 2009).

As for several chromatin-related proteins, the MYST–ING complexes comprise diverse subunits that carry various histone recognition modules that bind to different post-translationally modified residues. Indeed, they contain chromodomains, bromodomains, and PWWP domains, but the most abundant histone-binding domain found within these proteins is the PHD (plant homeodomain) finger. PHD fingers form a versatile recognition motif family that binds to different histone modifications of the N-terminal tail of histone H3. Most of the PHD fingers can read the histone methylation state of H3K4 (me0 vs. me2/3), but some can recognize other histone H3 residues and/or modifications (Musselman et al. 2012). We recently characterized the binding properties of the different PHD fingers found in the MYST acetyltransferase complex HBO1 (Saksouk et al. 2009; Avvakumov et al. 2012). Even though the various domains found within the complex have unique recognition motifs, we showed that they cooperate to bind chromatin on H3K4me3, a mark found near the transcription start sites (TSSs) of actively transcribed genes (Shilatifard 2006). The two PHD fingers of the JADE1L scaffold subunit (Fig. 1B) work together to recognize unmethylated H3K4, while the PHD finger of the ING4 subunit directs the binding of the entire complex toward H3K4me3. Indeed, ING tumor suppressor proteins all contain a PHD finger that recognizes H3K4me3 (Pena et al. 2006; Shi et al. 2006; Champagne et al. 2008; Saksouk et al. 2009). The integration of the different binding properties of PHD fingers within the HBO1 complex allows for its tumor suppressor activity through its regulation of transcriptional activity, leading to the control of cell proliferation (Avvakumov et al. 2012).

The BRPF1 protein is the scaffold subunit of the MYST acetyltransferase complex MOZ/MORF (Doyon et al. 2006; Ullah et al. 2008). It has been shown to play a role in maintaining anterior HOX gene expression during zebrafish development and consequently in determining segmental identity (Laue et al. 2008). It is also thought to be part of the TrxG family of genes, which are important for maintaining active genes during development (Laue et al. 2008). The mutually exclusive catalytic subunits of the complex (MOZ and MORF) are also known to play a role in HOX gene expression and development in both mice and zebrafish (Miller et al. 2004; Voss et al. 2009; Qiu et al. 2012). Moreover, the MOZ acetyltransferase is frequently translocated in acute myeloid leukemia and is required for proper hematopoietic stem cell (HSC) proliferation (Katsumoto et al. 2006; Thomas et al. 2006; Perez-Campo et al. 2009; Aikawa et al. 2010). As for many chromatin-related proteins, BRPF1 contains a variety of histone recognition modules that can bind to different modifications (Fig. 1B). Its N-terminal region has two PHD domains linked by a Zn knuckle (PZP [PHD–Zn knuckle–PHD] domain), while the C terminus has both a bromodomain and a PWWP domain. This PWWP domain can bind to the H3K36me3 mark found on the coding regions of active genes (Vezzoli et al. 2010). As for other scaffold subunits within MYST complexes, BRPF1 also contains at its N terminus a region of homology with the EPcA domain found in EPC proteins (Stankunas et al. 1998; Avvakumov et al. 2012). We showed that two homology subdomains within EPcA serve as docking sites—one for the HAT subunit (domain I) and one for the hEaf6 and ING proteins (domain II) (Fig. 1B; Avvakumov et al. 2012).

In this study, we first dissected the molecular interactions of the PZP domain in BRPF1 for different chromatin modifications, showing that the first PHD domain acts dominantly over the second one in targeting unmethylated H3K4, but they function together to drive binding to chromatin. Moreover, we found that the different subunits of the complex are distributed genome-wide over H3K4me3-rich regions, targeted by the ING5 subunit. Finally, we discovered that the different scaffold subunits of MYST–ING complexes not only play an essential role in enabling chromatin acetylation, but also select which histone tail is modified. We propose a model in which the HBO1 acetyltransferase is competing for binding to either BRPF or JADE scaffold subunits in cells and where this differential association determines which histone tail is acetylated by the HAT on chromatin. While JADE directs the acetylation toward the H4 tail, BRPF1 targets H3 acetylation. Our results thus provide novel insights into the mechanism by which MYST acetyltransferases target chromatin acetylation from yeast to human cells and thus help us to understand how these enzymes regulate their different cellular functions.

Results

The PZP domain of BRPF1 binds to unmethylated histone H3K4

BRPF1 contains many potential chromatin recognition domains, as depicted in Figure 1B. We previously demonstrated that the JADE1L scaffold subunit found within the HBO1 HAT complex contains a PZP domain that recognizes unmethylated H3K4 (Saksouk et al. 2009; Avvakumov et al. 2012). Importantly, the first PHD domain of BRPF2 (also known as Brd1, a paralog of BRPF1) has recently been shown to bind the N-terminal tail of histone H3 (Qin et al. 2011; Liu et al. 2012). As BRPF1 also contains a similar tandem PHD finger module, we characterized its affinity for histone marks. We first examined the affinity of the two separated PHD fingers using peptide pull-down experiments with recombinant domains fused to GST and biotinylated peptides (Fig. 1C). The first PHD (PHD1) domain shows specific binding to unmethylated H3K4 peptides, while the second PHD (PHD2) domain shows some interaction with H3 peptides irrespective of their methylation status. These interactions were also analyzed using nuclear magnetic resonance (NMR). Substantial chemical shift changes observed in the spectra upon addition of the peptide indicated that the PHD1

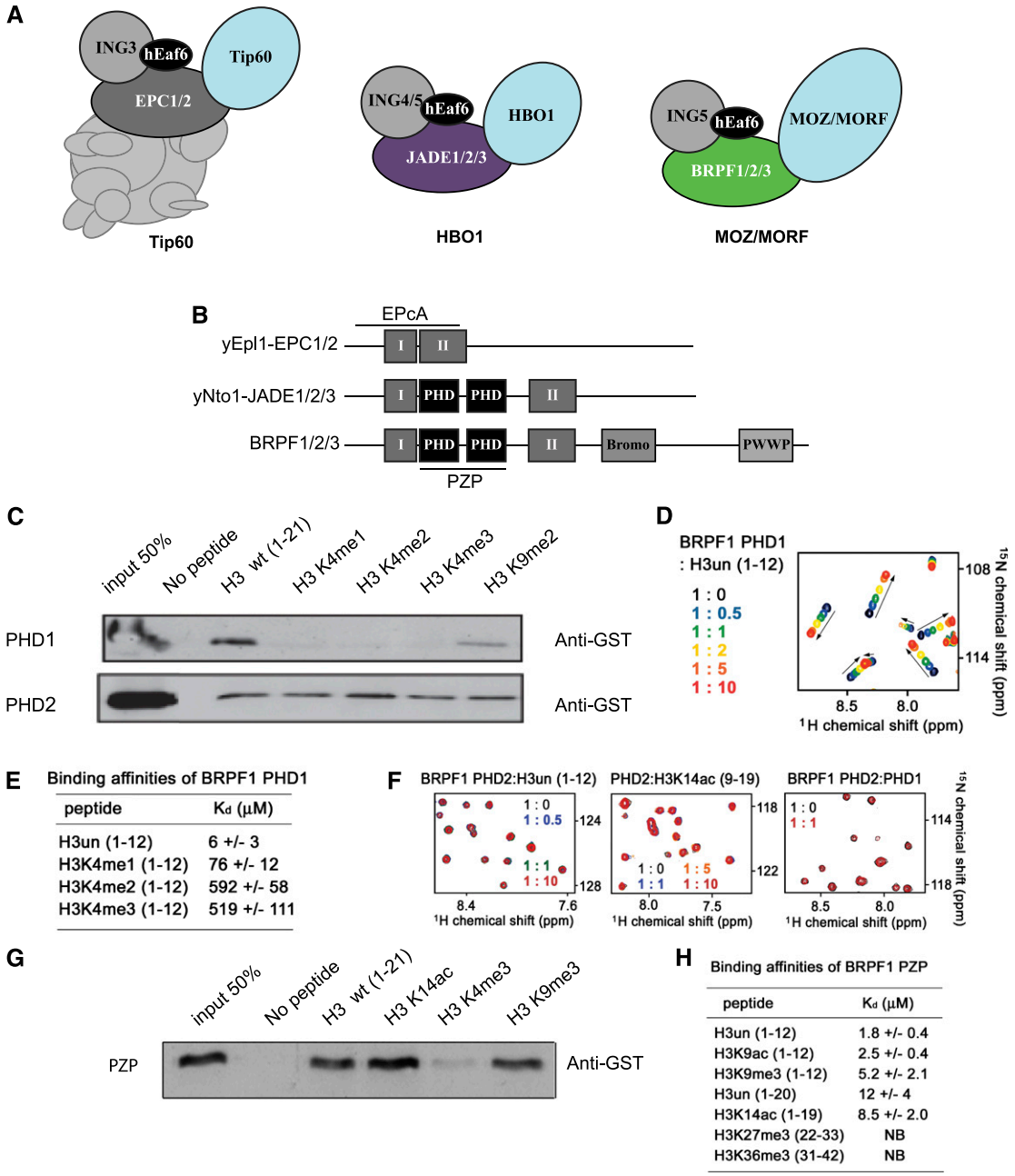

Figure 1. Characterization of the two PHD fingers in the PZP domain of BRPF1. (*A*) Subunit organization of human MYST acetyltransferase complexes used in this study. The core subunits have a scaffold protein (JADE, BRPF, or EPC), an ING tumor suppressor protein (ING3, ING4, or ING5), and a catalytic enzyme protein (Tip60, HBO1, or MOZ/MORF). (*B*) Schematic representation of the conserved protein domains found in the scaffold subunits of MYST–ING HAT complexes (yeast and human). (*C*) The PHD1 finger of the PZP domain of BRPF1 recognizes unmethylated H3 in vitro, while the PHD2 finger shows interaction with H3 peptides independently of methylation status. Peptide pull-down assays with different biotinylated peptides and recombinant PHD fingers fused to GST were analyzed by Western blotting with anti-GST antibody (Western blott: α-GST). (*D*) Superimposed $^{1}H,^{15}N$ heteronuclear single quantum coherence (HSQC) spectra of BRPF1 PHD1, collected as unmodified H3 peptide, was titrated in. The spectrum is color-coded according to the protein–peptide ratio. (*E*) Binding affinities of the BRPF1 PHD1 finger for histone H3 peptides with different K4 methylation statuses were measured by tryptophan fluorescence. Numbers in parentheses represent the amino acid positions of histone H3 included in the peptides. (*F*) Superimposed $^{1}H,^{15}N$ HSQC spectra of BRPF1 PHD2 (collected as indicated) peptides or unlabeled BRPF1 PHD1 were added stepwise. The spectra are color-coded according to the protein–peptide ratio. (*G*) The PZP domain of BRPF1 binds to unmethylated histone H3K4 in vitro. Peptide pull-down assays with different biotinylated peptides and recombinant PZP domain fused to GST were analyzed by Western blot with α-GST antibody. The PHD1 dictates the specificity of the entire domain toward unmethylated H3K4. (*H*) Binding affinities of the PZP domain for the indicated H3 peptides were measured by tryptophan fluorescence. Numbers in parentheses represent the amino acid positions included in the peptides. (NB) No binding was detected.

finger recognizes the unmodified histone H3 tail (Fig. 1D). Moreover, methylation or acetylation of H3K9 did not affect binding of PHD1 to H3 (see Supplemental Fig. 1a,b). Likewise, binding of the PHD1 finger to the histone peptides mono-, di-, and trimethylated at Lys4 was examined by tryptophan fluorescence (Fig. 1E). A single methyl group attached to Lys4 reduced binding of the PHD1 finger by ~10-fold, whereas affinity for H3K4me2 and H3K4me3 was dropped by ~100-fold. Thus, methylation of Lys4 disrupts the association of BRPF1 PHD1 with histone H3. Additionally, PHD1 requires the first N-terminal amino acids of the H3 tail for proper binding (see Supplemental Fig. 1b). These results indicate that PHD1 associates with the extreme N terminus of histone H3, likely through hydrogen bonds and ionic interactions with Ala1, Arg2, and unmodified Lys4, as reported for other PHD fingers (Musselman et al. 2012), and that this binding is disrupted by methylation of Lys4. To demonstrate that PHD1 has a mechanism of interaction similar to those of other H3K4me0-binding PHD fingers, we mutated two key conserved residues and measured significantly lower binding in peptide pull-down assays (Supplemental Fig. 1c,d).

Conversely, neither the N-terminal part of the histone tail (residues 1–12) nor the downstream sequence (residues 9–19) was able to induce chemical shift changes in the ^{15}N-labeled PHD2 finger of BRPF1, illustrating that this module alone is not capable on its own of specific binding to these sections of the histone H3 tail (Fig. 1F). We also found that PHD2 and PHD1 do not interact with each other, as no resonance perturbations were observed in the PHD2 finger during gradual addition of unlabeled PHD1 (Fig. 1F). On the other hand, nice chemical shift changes were obtained when incubating PHD2 with increasing amounts of deoxyribonucleoside monophosphates (dNMPs), suggesting that PHD2 could in fact interact with DNA (Supplemental Fig. 1e).

The two PHD fingers were then tested together as the full PZP module. Peptide pull-downs demonstrate that binding of the PZP to the N-terminal tail of H3 is inhibited by methylation of H3K4 (Fig. 1G), revealing PHD1 as a dominant recognition module over PHD2 within the PZP domain. To examine whether the Zn knuckle and/or the second PHD2 finger cooperate with PHD1 in the association with H3 by recognizing the histone sequence downstream from Lys9, binding affinity of BRPF1 PZP for a longer peptide was measured by tryptophan fluorescence. We found that PZP binds to the peptide containing residues 1–20 of histone H3un with a K_d of 12 μM (Fig. 1H; Supplemental Fig. 1f). This value was comparable with the K_d value measured for the interaction of a single PHD1 module with the short H3un peptide (6 μM) (Fig. 1E). Furthermore, the PZP domain and PHD1 alone exhibited similar affinities toward the short H3un peptide (K_d = 2 μM and 6 μM, respectively). Methylation or acetylation of Lys9 or Lys14 had very little to no effect on the interaction of PZP with the short H3un peptide (Fig. 1H; Supplemental Fig. 1f). Together, these data demonstrate that the PZP domain of BRPF1 recognizes the histone H3 N terminus that is unmethylated on Lys4 and that this in vitro interaction is driven by the first PHD.

Each PHD finger of the PZP domain is critical for chromatin binding and acetylation

To determine the functional relevance of the second PHD finger, we immunopurified wild-type and ΔPHD2 BRPF1 complexes from cotransfected 293T cells. Western analysis of the wild-type complex indicates the copurification of endogenous histone H3 (Fig. 2A). This cofractionation is completely lost after removal of the PHD2 domain of BRPF1, implying a crucial role in binding histone H3 in vivo. Furthermore, when the purified complexes were used in HAT assays, acetylation of chromatin was abolished by the deletion of PHD2, while acetylation of free histones was not affected (Fig. 2B). These data indicate that, while the NMR studies did not support a role in binding to the H3 tail, the second PHD of the PZP domain is essential for binding to chromatin and its subsequent acetylation. In order to compare these observations with the deletion of the first PHD domain, which drives the in vitro interaction, we then immunopurified both ΔPHD1 and ΔPHD2 complexes (Fig. 2C) and compared their acetyltransferase activity on chromatin and free histones. Similar to PHD2, the PHD1 finger is essential for acetylation of chromatin by the complex while not affecting acetylation of free histones (Fig. 2D,E). Altogether, these data demonstrate that both PHD fingers of BRPF1 are necessary for the complex to bind and acetylate chromatin, suggesting that the PZP domain functions as a single module binding to nucleosomes.

ING5 directs BRPF1 localization to H3K4me3-enriched chromatin at the 5′ end of active genes

We previously identified ING5 as the ING tumor suppressor subunit of the MOZ/MORF complexes (Doyon et al. 2006; Ullah et al. 2008). This association occurs via the conserved domain II of BRPF proteins (Ullah et al. 2008; Avvakumov et al. 2012). As ING proteins contain a PHD domain in their C termini that has been shown to recognize H3K4me3 (Pena et al. 2006; Champagne et al. 2008; Musselman et al. 2012), we asked whether the presence of the ING5 protein within the complex is targeting BRPF1 to the H3K4me3 mark in chromatin. First, we used recombinant complexes purified from SF9 cells ± ING5 to perform HAT assays on histone peptides. We observed that the HAT activity of the ING5-containing complex is greatly stimulated on H3K4me3 peptides when compared with unmodified or H3K9me peptides (Fig. 3A). This is reminiscent of our previous observations for ING4 and the JADE1/HBO1 complex, where the presence of ING4 stimulated acetylation of H3K4me3 peptides (Saksouk et al. 2009; Avvakumov et al. 2012). On the other hand, we observed a clear inhibition of HAT activity when peptides carry methylated Lys4 and ING5 is absent from the BRPF1 complex (Fig. 3B). This result corroborates what we observed in Figure 1G, where the PZP domain of BRPF1 is unable to bind H3 peptides that are methylated on Lys4. Together, these data suggest that there is an interplay between the different PHD domains found within the complex and that the PHD of ING5 is prevailing over the others in driving interaction with

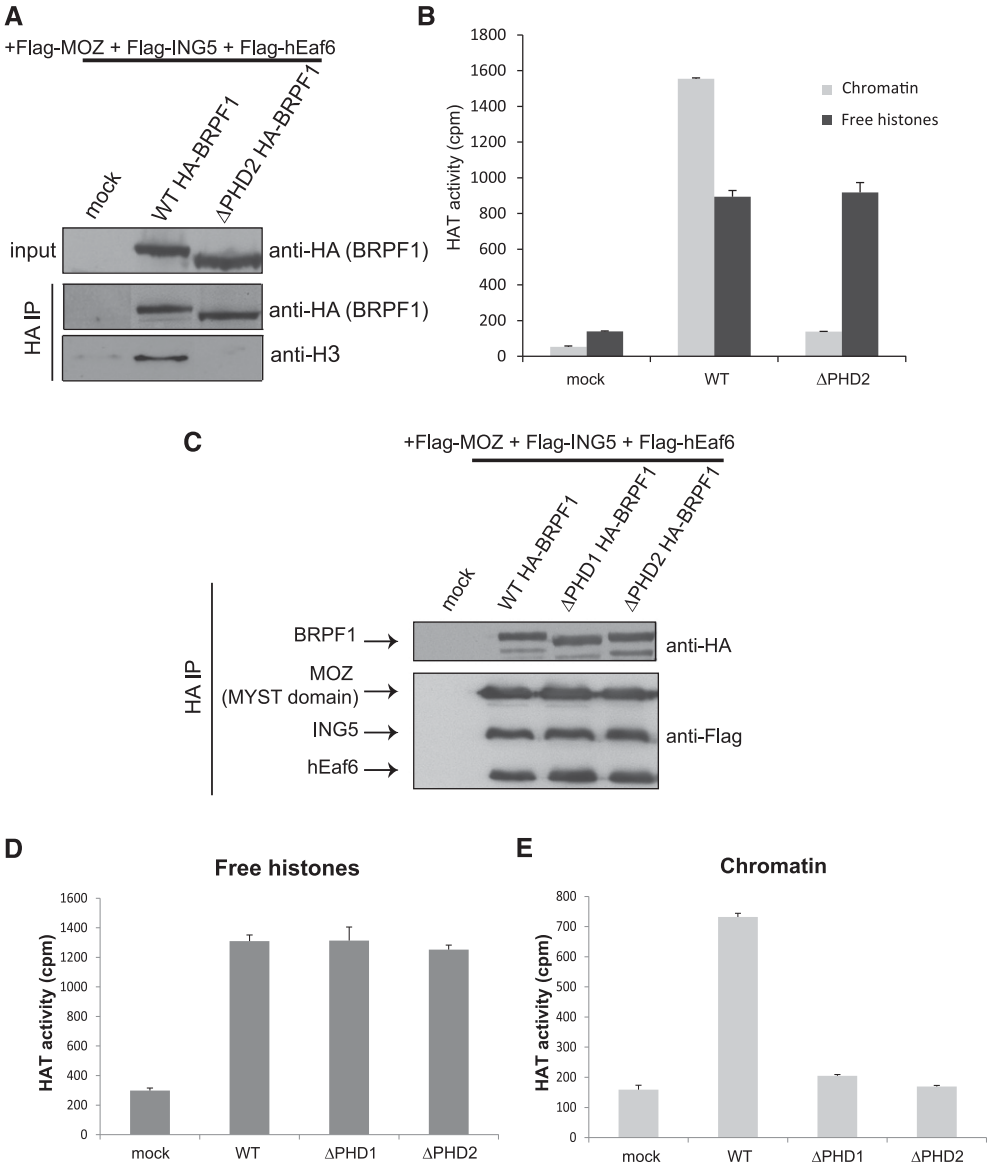

Figure 2. BRPF1 PHD1 and PHD2 fingers are required for binding to chromatin and its acetylation. (*A*) BRPF1 associates with histone H3 in vivo, and this binding is lost when the PHD2 finger is deleted. 293T cells were cotransfected with HA-BRPF1 (wild-type [WT] or ΔPHD2) plasmids, and Flag-MOZ (MYST domain), Flag-ING5, and Flag-hEaf6 plasmids and whole-cell extracts (WCEs) were used for HA immunoprecipitation (IP). As the MYST domain of the MOZ catalytic subunit is sufficient for HAT activity and complex assembly (Ullah et al. 2008), it was used to avoid the high degradation sensitivity of the full-length protein (225 kDa). Mock control was cotransfected with both HA empty and Flag empty plasmids. Histone H3 binding was analyzed by Western blot α-H3. (*B*) PHD2 is required for proper in vitro chromatin acetylation. HAT assays with the same purified complexes as in *A* were performed on chromatin or free histones. Reactions were spotted on membranes and counted by liquid scintillation. Values are based on three independent experiments with standard error. (*C*) Western blot on purified wild-type, ΔPHD1, and ΔPHD2 complexes in 293T cells showing equal expression of the different subunits. WCE was used after cotransfection of HA-BRPF1 plasmids (wild type, ΔPHD1, or ΔPHD2), and Flag-MOZ, Flag-ING5, and Flag-hEaf6 plasmids were used for HA immunoprecipitation. HA beads were eluted with HA peptide, and fractions were loaded on gel. (*D*,*E*) PHD1 is also important for acetylation of chromatin in vitro. HAT assays on free histones (*D*) or chromatin (*E*) using the complexes purified in *C* were spotted on membranes for liquid scintillation counting. Values are based on three independent experiments with standard error.

H3K4me3, while the BRPF1 PZP domain is required for binding to chromatin per se.

To test how this interplay occurs in vivo, we then performed chromatin immunoprecipitation (ChIP) combined with deep sequencing (ChIP-seq) experiments in human RKO cells using H3K4me3, ING, and BRPF antibodies. This p53-positive human colon carcinoma cell line shows the expected features when mapping the H3K4me3 chromatin mark; i.e., enrichment near the TSSs of active genes, with signals increasing with the

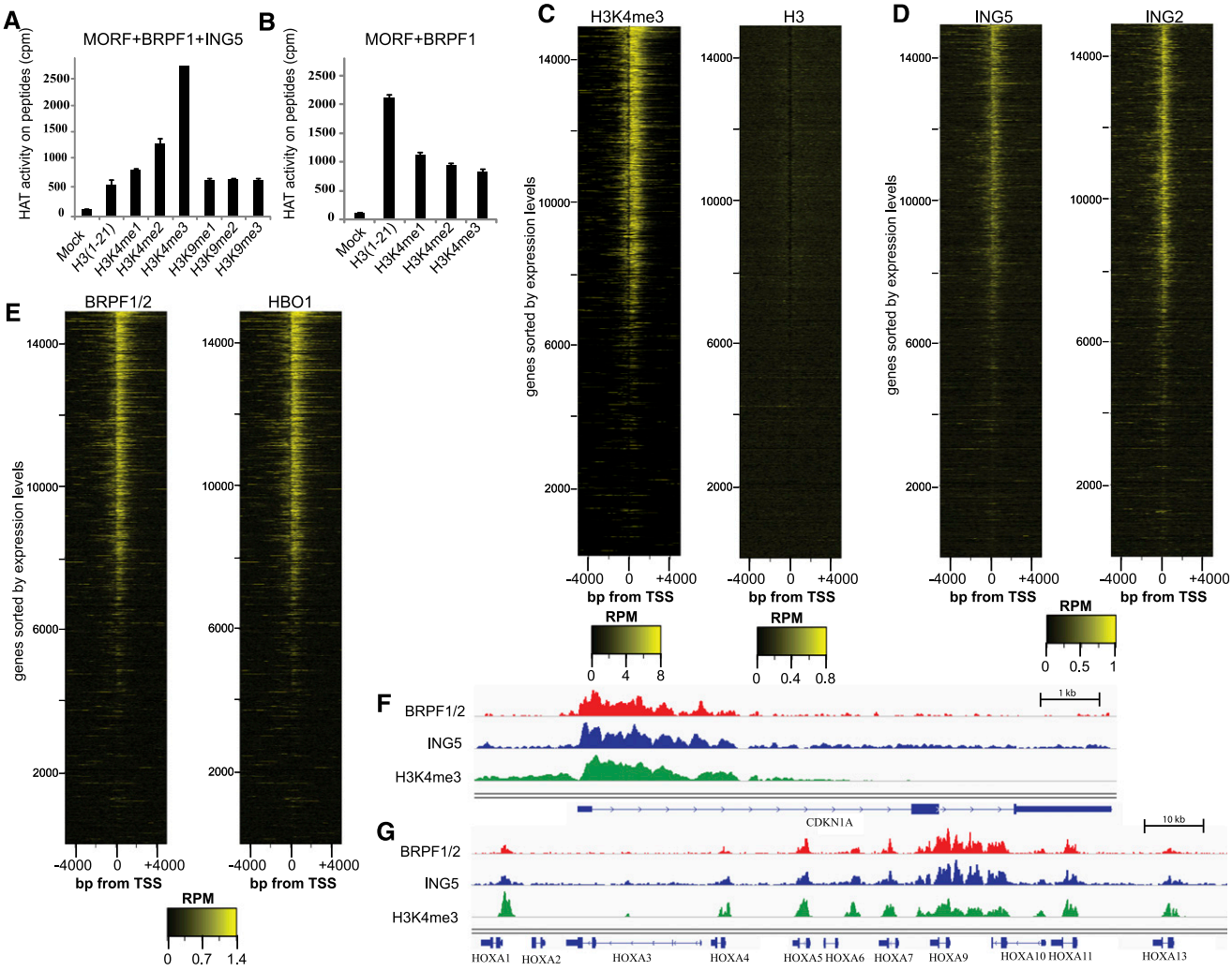

Figure 3. BRPF1 localizes to H3K4me3-enriched regions through its association with ING5. (*A*,*B*) ING5 directs the binding of the entire MORF complex toward H3K4me3 in vitro. Complexes ± ING5 were purified from SF9 cells and used in HAT assays on diverse modified histone peptides. Values are based on two independent experiments with standard error. (*C*–*E*) ING5, ING2, BRPF1/2, and HBO1 colocalize with H3K4me3 near the TSSs of genes. Heat maps of each protein ChIP-seq signal on ±5 kb surrounding the TSSs of genes are shown. Genes were sorted by gene expression level (see the Materials and Methods) from high (*top*) to low (*bottom*), and the signals were corrected over reads per million (RPM). (*C*) Enrichment of H3K4me3 signal compared with H3 signal. ING5 and ING2 (*D*) and BRPF1/2 and HBO1 (*E*) are bound at H3K4me3-enriched regions near the TSSs of genes. (*F*,*G*) BRPF1/2 and ING5 colocalize at the p21/CDKN1A gene and the HOXA cluster. The different signals for each protein are shown to illustrate their binding at H3K4me3-enriched region near the p21/CDKN1A TSS (*F*) and each TSS of the HOXA cluster (*G*).

expression levels (Fig. 3C; Supplemental Figs. 2a, 3). Genome-wide localization analysis of the ING5 protein showed enrichment around the TSSs of active genes, on the same regions where H3K4me3 is located (Fig. 3D; Supplemental Fig. 2b). In comparison, the ING2 protein, which also binds H3K4me3 through its PHD domain (Pena et al. 2006; Shi et al. 2006), was found within the same genomic regions (Fig. 3D; Supplemental Fig. 2c). ING2 is a subunit of the histone deacetylase (HDAC) complex mSin3a (Doyon et al. 2006; Shi et al. 2006). Our data indicate that ING5 (HAT) and ING2 (HDAC) complexes colocalize at the TSSs of actively transcribed genes, arguing for a primary role of their H3K4me3-binding PHD finger in this targeting. Previous genome-wide mapping of several HAT and HDAC proteins showed that they are similarly found near TSSs of actively transcribed regions in a dynamic process allowing rapid resetting of chromatin (Wang et al. 2009). We then used an antibody raised against the BRPF2 paralog to evaluate genomic distribution by ChIP-seq. This antibody is equally efficient at recognizing the BRPF1 protein (but not BRPF3) because of the highly conserved region used as an antigen (Supplemental Fig. 4). The BRPF1/2 distribution was also localized near the TSSs of active genes at H3K4me3-enriched regions, similar to what was observed for ING5 (Fig. 3E; Supplemental Fig. 3d). This is also almost identical to our recently published genome-wide profile of the HBO1 HAT in the same cell line (cf. heat maps in

Fig. 3E; Avvakumov et al. 2012). Upon closer examination at specific loci, we clearly observe colocalization of BRPF1/2 and ING5 proteins over H3K4me3-rich regions near the p21(CDKN1A) TSS and at the HOXA cluster (Fig. 3F,G).

Overall, these results show that BRPF1/2, ING5, and HBO1 proteins colocalize on H3K4me3-rich regions surrounding the TSSs of actively transcribed genes and that their signals are proportional to the expression level of these genes. In addition, it indicates that the ING5 protein is a primary determinant for BRPF1/2 complex association with specific genomic loci, correlating with its binding to the H3K4me3 histone mark both in vitro and in vivo.

Two distinct forms of HBO1 complexes exist with different scaffold subunits

We showed previously that the ING5 protein is associated with two different MYST acetyltransferase complexes in HeLa cells: the HBO1–JADE1/2/3 and MOZ/MORF–BRPF1/2/3 complexes (Fig. 1A; Doyon et al. 2006). A recent study in K562 cells argued that the BRPF2 scaffold protein could be associated with the HBO1 HAT (Mishima et al. 2011). To investigate this possible distinct interaction, we purified BRPF1 from stably transduced HeLa cells (Fig. 4A). Mass spectrometry and Western blot analyses confirmed association of MOZ/MORF HATs, hEaf6, and ING5, as we reported previously (Fig. 4A,B; Doyon et al. 2006; Ullah et al. 2008). Significant signals were also obtained for HBO1. Thus, both MOZ/MORF and HBO1 catalytic HAT subunits can be associated with BRPF1 in vivo. In addition, ING4 was also identified as a BRPF1-associated factor, in contrast to our previous results that suggested its restriction to HBO1–JADE1/2/3 complexes (Doyon et al. 2006). Moreover, using transduced HBO1 as bait for purification from HeLa cells, we were able to identify by Western blot and mass spectrometry both JADE1L and BRPF2/3 as interacting partners (Fig. 4C; data not shown). We also confirmed the interaction in 293T cells, where immunoprecipitation of Flag-HBO1 brings down endogenous BRPF1/2 proteins (Supplemental Fig. 5). These results demonstrate the presence of a new MYST–ING acetyltransferase complex within HeLa cells, formed by HBO1 and a BRPF paralog.

BRPF1–MYST complexes acetylate only histone H3 in chromatin

We used the purified BRPF1 fraction for in vitro HAT assays and observed a striking specificity for histone H3 in chromatin, while both H3 and H4 are targeted as free histones (Fig. 4D). While we previously found MOZ/MORF–BRPF–ING5 complexes to have similar specificity (Doyon et al. 2006; Ullah et al. 2008), the presence of HBO1 in the fraction suggested otherwise. Indeed, HBO1 is known to acetylate mainly the N-terminal tail of histone H4 on chromatin both in vitro and in vivo, specifically on Lys5, Lys8, and Lys12 (Doyon et al. 2006). We then used ChIP assays to determine whether the presence of additional BRPF1 protein in the transduced HeLa cells influences the level of H3 and H4 acetylation at specific loci in vivo. When compared with cells transduced with an empty vector, the Flag-BRPF1 cell line shows a significant increase of H3 acetylation on both Lys14 and Lys23 at the p21 TSS (Fig. 4E,F). Moreover, a slight increase can also be observed 2 kb downstream from the p21 TSS, where the BRPF1 complex is still likely bound (see Fig. 3F). We also noticed some increase of H4 acetylation at the same loci, but the effect seems much smaller and could be indirect/subsequent to H3 acetylation (Fig. 4G). Indeed, H3K14ac was recently shown to inhibit demethylation of H3K4 (Maltby et al. 2012), which would favor recruitment of other HATs through increased H3K4me3. Importantly, no change in H3 and H4 acetylation levels was observed at an intergenic control locus (Fig. 4E–G). These data indicate that purified BRPF1 complexes target mainly H3K14 and H3K23 in chromatin in vitro and in vivo despite the fact that a previously characterized H4-specific MYST enzyme, HBO1, is present in the fraction. However, HBO1 occupancy measured by ChIP on the same regions did not show any increase in BRPF1 transduced cells compared with the control cell line (Fig. 4H). This indicates that while increased BRPF1 level leads to higher H3 acetylation on p21, it does not seem to target additional HBO1 protein.

The scaffold subunits of the MYST–ING complexes direct histone tail specificity during acetylation of chromatin

Since no H4 acetylation was observed in vitro with the purified BRPF1 complexes containing either MOZ, MORF, or HBO1 catalytic subunits, we sought to determine the histone lysine residues targeted by the newly identified HBO1–BRPF1–ING5–hEaf6 complex. For this purpose, we overexpressed in 293T cells the different combinations of the desired subunits and purified the resulting complexes using the Flag-tagged scaffold subunit (Fig. 5A). These overexpressed complexes were then used in HAT assays on both free histones and chromatin. As expected, the BRPF1–MOZ complex acetylates H3 on chromatin, whereas the JADE1–HBO1 complex acetylates H4 (Fig. 5B). This is in sharp contrast to the lack of histone specificity when using free histones as the substrate, where histones H3/H4 are acetylated equally by both complexes. Remarkably, when the HBO1 acetyltransferase is associated with BRPF1, acetylation of chromatin by this complex is restricted to histone H3 (Fig. 5B). To more precisely identify the lysine residues acetylated on H3, we performed HAT assays with unlabeled acetyl-CoA followed by Western blot analysis with specific histone mark antibodies. We observed an increase in H3K23ac and H3K14ac with the HBO1–BRPF1 complex compared with the mock fraction, while no change in H3K9ac was detected (Fig. 5C). This H3K14/23 specificity was also observed using peptides in HAT assays (Supplemental Fig. 6). These results indicate that HBO1 can acetylate both H3 and H4 lysine residues on

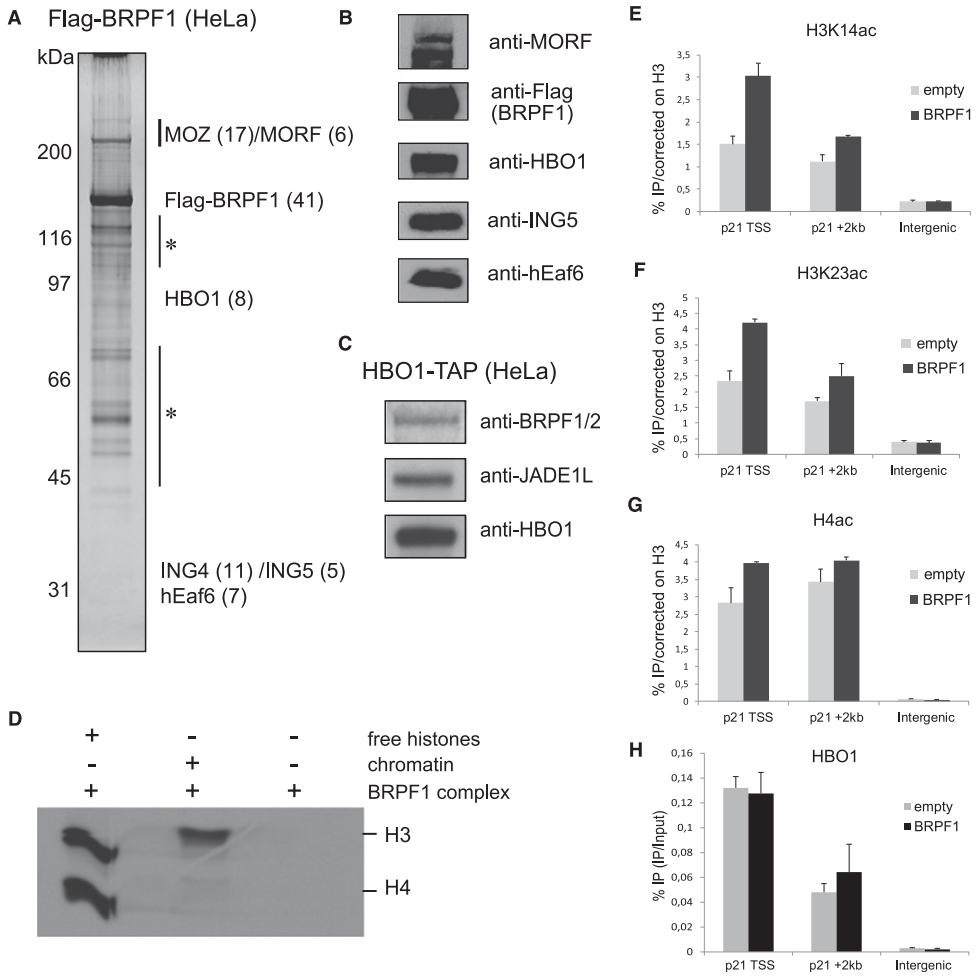

Figure 4. The BRPF1 scaffold subunit copurifies with both MOZ/MORF and HBO1 catalytic subunits. (*A*) A transduced stable HeLa cell line expressing 3xFlag-BRPF1 was used to purify associated proteins by anti-Flag immunoprecipitation/elution. Immunopurified proteins were analyzed on gel by silver staining. Nonspecific contaminants are shown by the asterisk. (*B*) The purified complex in *A* was analyzed by Western blot with the indicated antibodies. The two bands appearing with the MORF antibody are both MOZ and MORF, as the MORF antibody recognizes both proteins (Ullah et al. 2008). (*C*) Western blot analysis of a tandem affinity purification (TAP) from a transduced HeLa cell line stably expressing HA-HBO1-TAP (protein A and calmodulin-binding protein). (*C*) BRPF1 complexes acetylate histone H3 on chromatin in vitro. HAT assays were performed on free histones or native chromatin with the purified BRPF1 fraction in *A*. Acetylated histones were separated by SDS-PAGE and revealed by fluorography. (*E–G*) BRPF1 complexes acetylate histone H3 on chromatin in vivo. ChIP analysis of H3K14/K23 and H4 acetylation in transduced HeLa cells stably expressing BRPF1. Acetylation levels corrected for nucleosome occupancy (total H3 signal) were measured at the p21 TSS, 2 kb downstream, and at an intergenic locus. BRPF1 significantly increases H3K14ac and H3K23ac at the p21 TSS while showing no effect at the intergenic locus. (*H*) HBO1 occupancy on p21 gene does not change upon increased BRPF1 expression. ChIP analysis of HBO1 in BRPF1 and control transduced cell lines. All ChIP values are based on two independent experiments with standard error.

chromatin but that its specificity is determined by the associated scaffold subunit. While HBO1–JADE–ING–hEaf6 targets H4K5/8/12 on chromatin, HBO1–BRPF–ING–hEaf6 targets H3K14/23.

Since JADE and BRPF PZP domains behave similarly in histone/chromatin-binding functions (Figs. 1, 2; Saksouk et al. 2009; Avvakumov et al. 2012) and their domain II associates with the same set of ING proteins (ING4/5), the drastic change of nucleosomal histone specificity put on the MYST acetyltransferase must originate from other parts of these scaffold proteins. Obvious candidate features are present on BRPF proteins, since they also contain a Kac-binding bromodomain and a H3K36me3-binding PWWP domain at their C termini (Fig. 1B; Vezzoli et al. 2010; Filippakopoulos et al. 2012). We constructed C-terminal deletions of the PWWP domain and the bromodomain in BRPF1. We purified HBO1 complexes containing either wild-type BRPF1 or BRPF1 lacking these domains (Fig. 5D) and used them in HAT assays (Fig. 5E). Neither the deletion of the PWWP domain nor the deletion of the bromodomain of BRPF1 affected the specificity of HBO1 for histone H3 on chromatin substrate. These data indicate that the two histone mark reader modules at the C terminus of BRPF1 are not

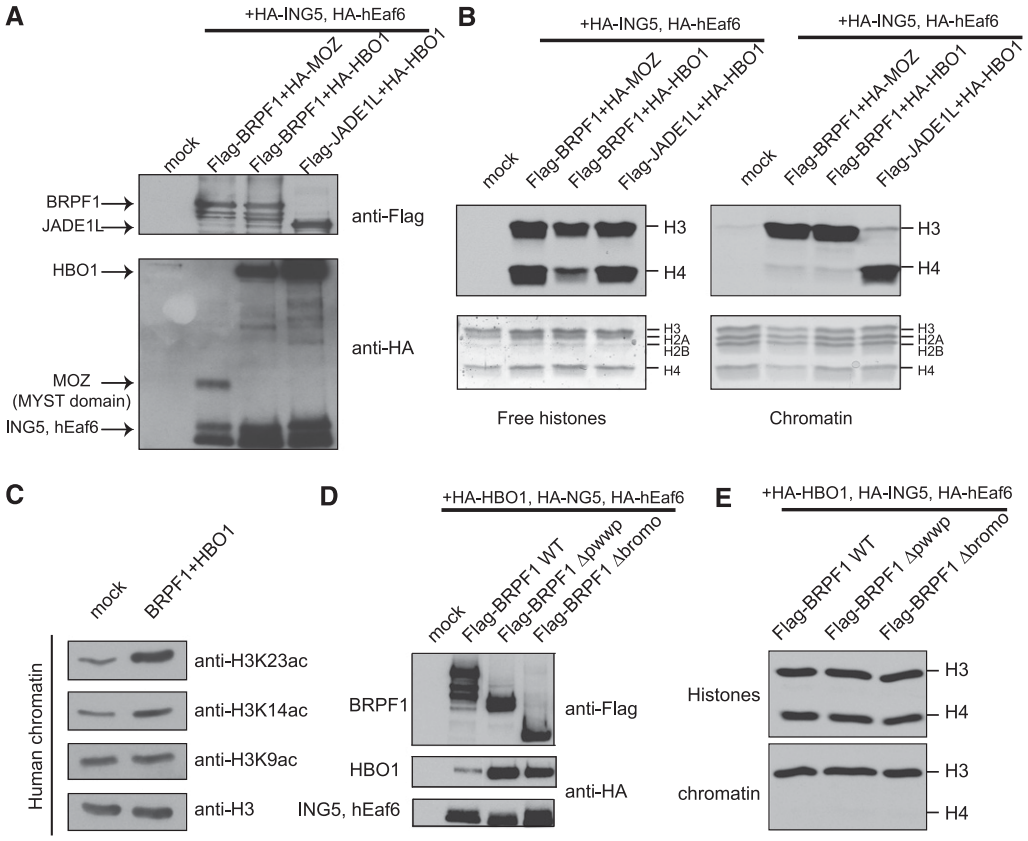

Figure 5. Association of different scaffold subunits with the HBO1 HAT is responsible for switching its histone acetylation specificity between H4 and H3. (*A*) Purification of the MOZ–BRPF1, HBO1–BRPF1, and HBO1–JADE1L complexes. 293T cells were transfected with flagged scaffold subunit plasmids (BRPF1 and JADE1L), while other cotransfected subunits were HA-tagged. Mock control was cotransfected with Flag empty and HA empty plasmids. Complexes were purified from WCEs by Flag immunoprecipitation (IP) and eluted with 3xFlag peptides. (*B*) The scaffold subunit changes chromatin acetylation specificity. The purified complexes in *A* were used in HAT assays on both chromatin and free histones. Acetylated histones were separated by SDS-PAGE and revealed by fluorography. Coomassie-stained gels show equivalent amounts of histones between samples. (*C*) The HBO1–BRPF1 complex acetylates H3K14 and H3K23. HAT assays with the purified HBO1–BRPF1 complex were performed on chromatin followed by Western blot analysis of different histone marks. (*D*) Purification of various deletions of Brpf1. Cotransfected 293T cells with either wild-type (WT), ΔBromo, or ΔPWWP Flag-BRPF1 plasmids combined with HA-HBO1, HA-ING5, and HA-hEaf6 plasmids were used for Flag immunoprecipitation purification, and complexes were analyzed by Western blot with the indicated antibodies. (*E*) The PWWP domain and bromodomain of BRPF1 are not essential for acetylation specificity. The purified complexes in *D* were used in HAT assays on both chromatin and free histones. The amount of complex used for HAT assays was normalized to free histone activity. Acetylated histones were separated by SDS-PAGE and revealed by fluorography.

involved in selecting the histone tail specificity of the HAT complex.

A short N-terminal region within scaffold subunits directs which histone tail is acetylated by MYST complexes on chromatin

When comparing sequence homologies between scaffold subunits of human MYST–ING HAT complexes, it became apparent that some features were conserved at the N-terminal region, just before the domain I, responsible for binding the MYST subunit (Fig. 6A). This region is considered part of the larger EPcA domain in EPC proteins, scaffold subunits of the NuA4/Tip60 HAT complex (Fig. 1A,B). We showed previously that this small region at the beginning of EPcA is important for chromatin binding and nucleosomal HAT activity of the yeast NuA4 complex (Selleck et al. 2005; Chittuluru et al. 2011). To investigate whether the corresponding N-terminal region in BRPF1 or JADE1 scaffold subunits is implicated in nucleosomal HAT activity and, perhaps, histone tail selection, we produced N-terminal deletions that removed the first 20 amino acids of the EPcA-related region. The wild-type or truncated JADE1 and BRPF1 scaffold subunits were purified as tetrameric complexes from cotransfections with either HBO1 or MOZ as the catalytic subunit. HAT assays with the purified complexes were performed on chromatin (Fig. 6B). Strikingly, association of MOZ with JADE1 instead of BRPF1 also shifts its histone tail specificity from H3 to H4, as we observed for HBO1 (Fig. 6B, cf. lanes 4 and 8 and lanes 2 and 6). Since MOZ is mostly known for acetylating

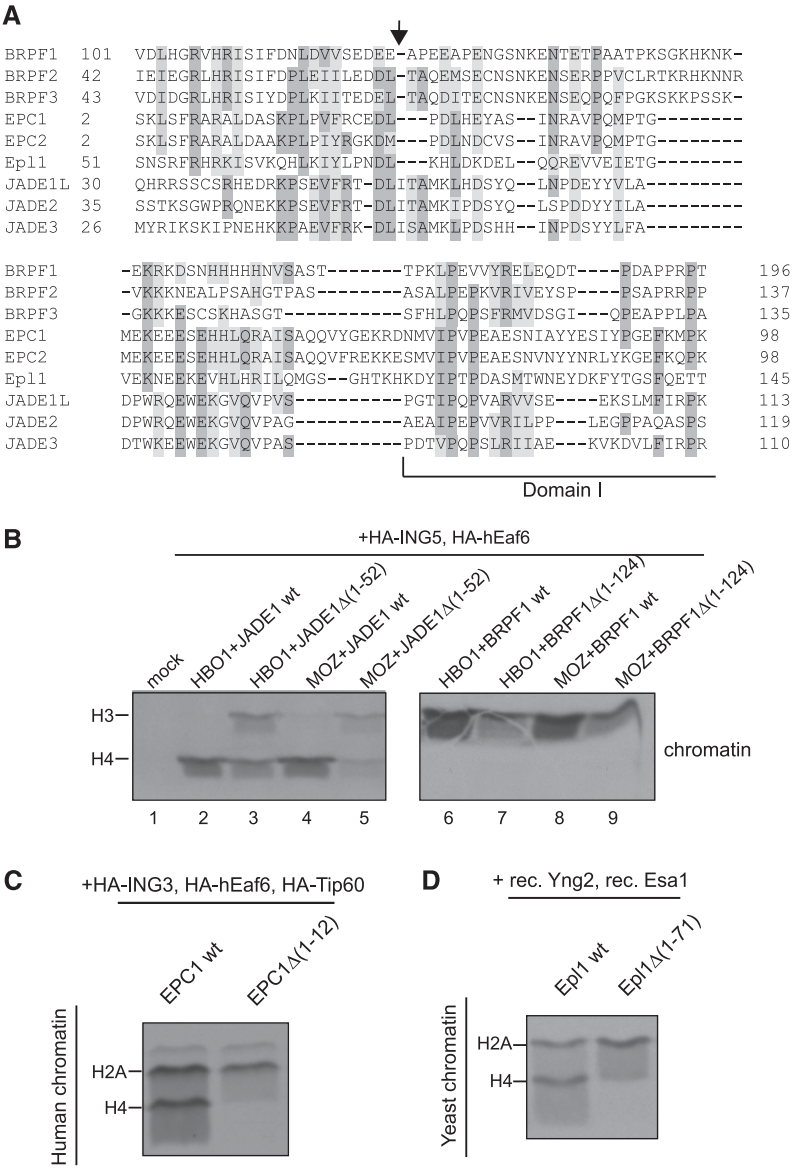

Figure 6. A small N-terminal domain in the scaffold subunits of the MYST–ING complexes is responsible for directing specific histone tail acetylation. (*A*) Sequence alignment of scaffold subunits of the MYST–ING complexes with the N-terminal region of the EPcA domain found in the EPC proteins (EPC1/2 and Epl1). An arrow indicates the location of the N-terminal truncation in BRPF1 and JADE1 mutants. Domain I is the region of association with the MYST HAT. (*B*) Deletion of the N-terminal part of scaffold subunits BRPF1 and JADE1L alters chromatin acetylation specificity. 293T cells were cotransfected with the indicated expression plasmids, HA-tagged catalytic subunits, and Flag-tagged scaffold subunits. HA-ING5 and HA-hEAF6 expression plasmids were also cotransfected for each purification. Flag immunoprecipitations (IPs) were performed on WCE and were eluted with 3xFlag peptides. Purified complexes were used in HAT assays, and acetylated histones were separated by SDS-PAGE and revealed by fluorography. The complexes were normalized to the same HAT activity on free histones (by liquid assays). (*C*) Deletion of the N-terminal part of scaffold subunit EPC1 also modifies chromatin acetylation specificity. EPC1 wild-type and Δ1–12 complexes were purified and used for HAT assays by coexpressing Flag-EPC1, HA-ING3, HA-hEaf6, and HA-Tip60. (*D*) The N-terminal domain of the yeast homolog Epl1 acts similarly in directing histone specificity. Recombinant yeast piccolo NuA4 complexes with wild-type or Δ1–71 Epl1 were used for HAT assays on yeast chromatin, and acetylated histones were treated as in *A*.

histone H3, this result clearly supports our previous conclusion about HBO1 and expands it to other MYST HATs; i.e., that it is the scaffold subunit that is responsible for directing the histone tail specificity during acetylation of chromatin, not the acetyltransferase subunit.

When associated with HBO1, removal of the small N-terminal EPcA-related region of JADE1 protein resulted in not only a loss of H4 acetylation on chromatin, but also a clear appearance of H3 acetylation (Fig. 6B, lanes 2,3). This was also the case when truncated JADE1 was associated with MOZ (Fig. 6B, lanes 4,5). These results indicate that this region of JADE1 is important for not only acetylation of chromatin, but also histone tail selection. However, removal of the same region in BRPF1, while leading again to a loss of HAT activity on chromatin for both HBO1 and MOZ, did not seem to significantly change histone tail specificity, as only H3 acetylation could be observed (Fig. 6B, cf. lanes 6 and 7 and lanes 8 and 9). However, repeating the assay with equivalent amounts of nucleosomal HAT activity between the wild-type and mutant complexes showed a significant loss of histone tail specificity, as H4 acetylation is now detected in the mutants (Supplemental Fig. 7). Thus, deletion of the EPcA-related region leads to reduced nucleosomal HAT activity, as we showed for yeast Epl1 in NuA4 (Selleck et al. 2005; Chittuluru et al. 2011). However, our results also indicate that the same region of JADE1 is indeed responsible for selecting the H4 tail versus H3 for acetylation on chromatin. Since the loss of tail specificity detected with the BRPF1 mutant is more subtle, it is possible that H3 tail acetylation is the default target driven by the PZP domain in JADE and BRPF proteins.

To further investigate the molecular mechanisms of histone tail selectivity, we analyzed other MYST–ING HAT complexes that contain scaffold subunits naturally lacking a PZP domain. We purified the human Tip60–

EPC1–ING3–hEaf6 complex from cotransfected cells and the recombinant yeast piccolo NuA4 complex from bacteria. Both of these complexes selectively acetylate histone H4 and H2A tails on chromatin substrates (Fig. 6C,D), while they can target H3 in free histones (Boudreault et al. 2003; Doyon et al. 2004). Removal of only the first 12 amino acids of human EPC1 and its EPcA domain completely abolishes acetylation of the histone H4 tail by Tip60 on chromatin (Fig. 6C). In a clear contrast, acetylation of the histone H2A tail is preserved. Similar results were obtained with yeast piccolo NuA4, as a complex containing the equivalent deletion of the yeast scaffold protein Epl1 also lost its activity toward nucleosomal histone H4 tail but retained its activity toward H2A (Fig. 6D). Thus, deletion of the first portion of the EPcA-related domain resulted in loss of H4 acetylation in Tip60/EPC1, NuA4/Epl1, JADE1/MOZ, and JADE1/HBO1 complexes, supporting a role for this domain in orienting the MYST HAT to acetylate the H4 tail in chromatin. However, since there was no loss of H2A tail-specific acetylation by Tip60 and NuA4, in comparison with gain of H3 tail acetylation in the case of JADE1, these results suggest that other histone tail specificity determinants are at play, likely within the same region of the scaffold subunits. Altogether, these data indicate that scaffold subunits in MYST acetyltransferase complexes are not only essential to enable acetylation of chromatin, but also required to direct which histone tail gets acetylated.

Discussion

Post-translational modifications of histone residues can directly alter chromatin structure by modulating the interactions between histones and DNA. They can also serve as docking platforms for the binding of chromatin-associated proteins and thus in activating nuclear signaling pathways (Musselman et al. 2012). A tight regulation of the deposited modifications and the related enzymes is thus necessary to ensure proper chromatin dynamics. The MYST family of acetyltransferases assembles in different multiprotein complexes. Several subunits of these complexes contain such histone recognition motifs (Avvakumov and Cote 2007b; Avvakumov et al. 2012). In this study, we dissected the binding properties of the PZP domain located in the BRPF1 protein, a scaffold subunit of MOZ/MORF HAT complexes. We found that, as for JADE1 and BRPF2 PZP domains (Saksouk et al. 2009; Qin et al. 2011; Avvakumov et al. 2012), the first PHD finger of BRPF1 has strong affinity for the histone H3 N-terminal domain but only when H3K4 is not methylated. Interestingly, PHD1 acts dominantly over PHD2 within the PZP in blocking interaction with methylated forms of H3K4 (Fig. 1). Nevertheless, both PHD1 and PHD2 are required for the MOZ–BRPF1–ING5–hEaf6 complex to bind histone H3 in vivo and acetylate chromatin in vitro (Fig. 2). Thus, although PHD2 does not show any structured binding to histone peptides in vitro, it is still required for proper binding of the BRPF1 complexes to chromatin. This is reminiscent of the JADE1 PHD2 finger, which is also essential for binding chromatin in vivo and for the tumor suppressor activity of the HBO1 complex (Saksouk et al. 2009). However, our results with BRPF1 PHD fingers suggest that they act together as a single functional module, the PZP domain, to bind chromatin and allow its acetylation by the MYST HAT. This is supported by similar results obtained when only the Zn knuckle region between PHD1 and PHD2 is deleted (data not shown). Interestingly, it was recently suggested that the BRPF2 PHD2 finger could in fact bind DNA (Liu et al. 2012). Our NMR data with dNMPs and BRPF1 PHD2 also support this model (Supplemental Fig. 1e). Thus, within the PZP domain, PHD2 could assist PHD1 by allowing binding to nucleosomal DNA, while PHD1 locks in the histone H3 N-terminal domain.

As multiple chromatin-binding domains are found within the different subunits of MYST–ING HAT complexes, further study is still required to understand the interplay that exists between them. We showed that the ING5 PHD domain directs binding of the associated complexes to H3K4me3-rich regions and stimulates acetylation both in vitro and in vivo (Figs. 3, 4). Since both MOZ and BRPF1 have been linked to HOX gene activation (Laue et al. 2008; Voss et al. 2009; Qiu et al. 2012), it is thus very likely that their transcriptional regulation occurs via their binding to the TSSs of these genes, which are highly enriched in H3K4me3 (Fig. 3G). Moreover, in the absence of ING5, we clearly demonstrate that the PZP domain-binding features inhibited the acetylation on H3K4 methylated peptides (Fig. 3B). Thus, the PHD of the ING5 subunit prevails over the PZP domain of BRPF1, redirecting the binding of the complex to H3K4me3-containing chromatin. Nevertheless, even when ING5 is present, the PZP domain is required for binding to chromatin and acetylation. It is possible that BRPF–ING HAT complexes target asymmetric nucleosomes in which only one H3 tail is methylated on Lys4. These complexes may also favor spreading of the H3K4 methylation mark by simultaneously binding a methylated nucleosome through ING5 and an adjacent unmethylated one through the PZP, leading to acetylation of H3K14, which stimulates methylation of H3K4 (Nakanishi et al. 2008; Maltby et al. 2012). The MOZ/MORF HATs found associated with BRPF1 also contain a tandem PHD domain that has recently been shown to bind unmodified H3R2 and acetylated H3K14 (Ali et al. 2012; Qiu et al. 2012). It will be interesting to determine how the five PHD fingers found in different subunits of the MOZ/MORF–BRPF1–ING5–hEaf6 complex functionally interact with each other and other histone reader modules during binding to chromatin.

Some apparent contradictions are present in the literature regarding the HBO1 acetyltransferase. We and others have shown that the HBO1 enzyme is purified with JADE scaffold proteins and is responsible for histone H4 tail acetylation (Doyon et al. 2006; Iizuka et al. 2006, 2008; Foy et al. 2008; Miotto and Struhl 2010). We even showed that HBO1 siRNA-mediated knockdown in HeLa cells leads to a global loss of H4 acetylation on Lys5, Lys8, and Lys12, matching in vitro specificity on chromatin and arguing that HBO1 was the main H4-specific HAT in

mammals (Doyon et al. 2006). On the other hand, it was later shown that HBO1 gene knockout in mouse embryos leads instead to a loss of bulk H3K14ac in primary embryonic fibroblasts at embryonic day 9.5 (E9.5), while H4 acetylation persisted (Kueh et al. 2011). In addition, a HBO1–BRPF2 complex was reported in K562 leukemic cells and shown to target global H3K14 acetylation and erythroid regulators (Mishima et al. 2011). These contradicting results are quite adequately explained in the present study with the finding that HBO1–JADE and HBO1–BRPF HAT complexes coexist within HeLa cells (Fig. 4). Moreover, this differential association with distinct scaffold subunits is responsible for switching HBO1 specificity on chromatin toward different histone tails (Fig. 5). The HBO1–JADE1 complex targets mainly H4 residues, whereas the HBO1–BRPF1 complex acetylates only H3 in the context of chromatin. The varying protein expression levels between different tissues and/or during different developmental stages thus allow for fine-tuned regulation, leading to differential patterns of acetylated histones across the genome. Such functionally important tissue-specific variability of paralog subunits in chromatin regulators has been well documented for the BAF(SWI/SNF) remodeling complex (Hargreaves and Crabtree 2011). It is important to point out that HBO1 is nevertheless confirmed as a major mammalian HAT, since its depletion leads to global loss of histone acetylation on H3 in mouse erythroblasts/embryonic fibroblasts or on H4 in HeLa cells (Doyon et al. 2006; Kueh et al. 2011; Mishima et al. 2011). It will be very interesting to determine what is responsible for bulk H4 acetylation in *Hbo1*$^{-/-}$ mouse embryonic fibroblasts (Kueh et al. 2011). Is it Tip60? Is it another MYST HAT now associated with a JADE protein?

We identified a short EPcA-related N-terminal domain in BRPF1 and JADE1 as the region responsible for histone tail specificity of the associated MYST acetyltransferase on chromatin substrates (Figs. 6, 7). Interestingly, truncation of this domain in human EPC1 and yeast Epl1 protein cripples Tip60/NuA4's ability to acetylate nucleosomal H4, but histone H2A acetylation persists. This basic region of Epl1 was recently shown in cross-linking experiments to bind the histone H2A N-terminal tail in nucleosomes (Huang and Tan 2013). Thus, it is tempting to speculate that this binding to H2A is orienting the NuA4 complex on the nucleosome to target the H4 tail for acetylation. The corresponding regions in BRPF and JADE proteins would bind nucleosomes in distinct manners, leading to different histone tail selection for acetylation. The residual acetylation of H3 tail detected in BRPF1 and JADE1 truncations may be driven by the H3-binding function of the PZP domain and/or the ING subunit. Indeed, we showed that H3K4me3-binding ING4/5 subunits favor acetylation of histone H3K14 even from within the HBO1–JADE1 complex (Hung et al. 2009; Saksouk et al. 2009). It is important to point out that ING4/5 in this case allows H3K14 acetylation on top of the main H4 acetylation performed by HBO1–JADE1, not a complete switch of histone tail specificity, as demonstrated here between the HBO1–JADE1 and HBO1–BRPF1 complexes.

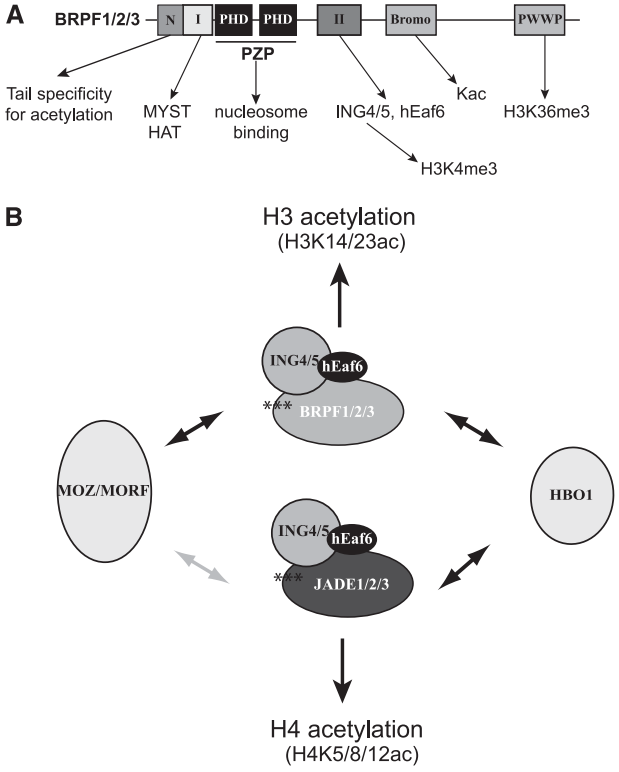

Figure 7. Model for MYST acetyltransferase assembly in alternate complexes, leading to different histone tail specificities. (*A*) Schematic representation of protein domains in BRPF paralogs and their demonstrated specific interactions/roles. (*B*) The HBO1 and MOZ/MORF catalytic subunits can be associated with different scaffold proteins, leading to a switch in histone tail specificity for acetylation of chromatin substrates. Thus, protein complexes associated with HAT proteins not only enable them to acetylate chromatin substrates, but also select which histone tail is targeted, a specificity previously thought to reside in the acetyltransferase itself. The arrow between MOZ/MORF and JADE1/2/3 is gray, since this interaction has only been reported in cotransfection experiments.

It is well established that acetylation neutralizes the charge of lysine residues to modulate the interactions with nucleosomal DNA and neighboring nucleosomes, regulating higher-order chromatin structure (Tse et al. 1998). Indeed, H3 acetylation shows distinctive effects on modulating the tertiary structure compared with H2A or H4 acetylation (Siino et al. 2003; Wang and Hayes 2008), underlying the importance of specific histone acetylation in regulating different cellular processes. H3 acetylation essentially appears to affect DNA accessibility in individual nucleosomes, while H4 acetylation has more long-range effects on chromatin compaction (Wang and Hayes 2008). Moreover, acetylated lysines on histones H3 and H4 can recruit distinct nuclear effector proteins, such as transcriptional coactivators like Rsc4 by H3K14ac, TRIM24 by H3K23ac, and Brd2 by H4ac (Agalioti et al. 2002; Kasten et al. 2004; Agricola et al. 2006; Tsai et al. 2010; Draker et al. 2012). Such differential recruitment of specific bromodomain-containing proteins could thus help regulate

the expression levels of specific genes (Filippakopoulos et al. 2012). It remains to be determined how the specific diacetylation of H3K14/23 by BRPF1–MYST complexes is interpreted compared with the different combinations deposited on H3 by PCAF/GCN5 and CBP/p300.

In conclusion, this study uncovers a new crucial role of factors associated with HAT proteins in multisubunit complexes. We and others demonstrated previously that complex assembly is required to enable HAT enzymes to acetylate their targets in native chromatin substrates (Carrozza et al. 2003). We now show that scaffold subunits associated with MYST family HATs not only allow chromatin binding and acetylation, but also select which histone tail becomes acetylated. Until now, histone tail specificity has been thought to reside in the acetyltransferase protein. The alternate association of the HBO1 catalytic subunit with BRPF and JADE proteins induces a striking shift of acetylation specificity between H3 and H4 tails. These results highlight the new role of the associated scaffold subunits within MYST–ING acetyltransferase complexes in directing the acetylation of specific histone tails. These findings add a new mechanism to the regulation of chromatin dynamics and call for caution when interpreting and comparing studies in which the function of HAT proteins is analyzed outside their physiological context.

Materials and methods

Purification of MYST HAT complexes

The native BRPF1 complex was purified from a retrovirus transduced HeLa cell line expressing 3xFlag-BRPF1 from a CMV promoter (pRCF vector). Nuclear extract were prepared following standard procedures (Abmayr 1993), and immunoprecipitation with anti-Flag agarose beads (Sigma) was done before eluting with Flag peptide buffer (100 mM KCl, 20 mM HEPES at pH 7.5, 20% glycerol, 0.1% Triton X-100, 400 μg/mL 3xFlag peptide, 1 mM DTT, 0.1 mM $ZnCl_2$, 1 mM PMSF). Tandem affinity purification of the native HBO1 complexes was done as previously described (Doyon et al. 2006). Purification of MYST complexes from transient transfections was performed in 293T cells. Cells were transfected near confluency with 6 μg of each plasmid (MYST, ING, BRPF/JADE/EPC, and hEAF6 with the indicated tags) per 150-mm plate. Cells were harvested 48 h post-transfection, and whole-cell extracts (WCEs) were prepared followed by anti-Flag immunoprecipitation/elution with Flag peptide or anti-HA immunoprecipitation/elution with HA peptide as previously described (Saksouk et al. 2009; Avvakumov et al. 2012). Tandem mass spectrometry analysis was done after in-gel digestion with trypsin at the Taplin Mass Spectrometry Facility. Expression vectors were constructed and, when indicated, mutated following standard procedures (details are available on request). PHD1 and PHD2 deletions correspond to amino acids 265–355 and 359–450.

Recombinant protein purifications and peptide pull-downs

The BRPF1 PHD1 (amino acids 275–329), PHD2 (amino acids 385–456), and PZP (amino acids 256–543) domains were expressed in *Escherichia coli* Rosetta pDEST15 or BL21 pGEX4T3 cells grown in LB or $^{15}NH_4Cl$ minimal medium supplemented with 1.5 mM $ZnCl_2$. After induction with 1.0 mM IPTG for 16 h at 20°C, bacteria were harvested by centrifugation and lysed with lysozyme and/or by sonication. The unlabeled and ^{15}N-labeled GST fusion proteins were purified on glutathione Sepharose 4B beads (GE Healthcare). The GST tag was either cleaved with PreScission protease or kept for Western blot analysis/peptide pull-downs, in which case the GST fusion protein was eluted off the glutathione Sepharose beads using 50 mM reduced L-glutathione (Sigma Aldrich). For NMR analysis, the proteins were concentrated into 20 mM Tris-HCl (pH 6.8) in the presence of 150 mM NaCl, 10 mM dithiothreitol, and 10% D_2O. Protein complex purification from bacteria and SF9 cells was done as previously described (Selleck et al. 2005; Ullah et al. 2008). Peptide pull-downs with GST fusion proteins were performed as previously described using biotinylated peptides and streptavidin magnetic beads (Saksouk et al. 2009).

NMR spectroscopy

NMR experiments were performed at 25°C on Varian INOVA 600- and 500-MHz spectrometers using pulse field gradients to suppress potential artifact and eliminate water signal. ^{1}H,^{15}N heteronuclear single quantum coherence (HSQC) spectra of uniformly ^{15}N-labeled PHD1, PHD2, and PZP (0.1–0.2 mM) were recorded as histone tail peptides (synthesized by the University of California at Davis Biophysics Core Facility), dNMPs (a mixture of dAMP, dTMP, dCMP, and dGMP, 1:1:1:1), or unlabeled PHD1 were added stepwise.

Fluorescence spectroscopy

Tryptophan fluorescence measurements were carried out at 25°C on a Fluoromax-3 spectrofluorometer. The samples of 1–10 μM PHD1 or PZP containing progressively increasing concentrations of histone peptides (up to 1 mM) were excited at 295 nm. Emission spectra were recorded between 305 and 405 nm with a 0.5-nm step size and a 1-sec integration time and were averaged over three scans. K_d values were determined by a nonlinear least-squares analysis using the equation

$$\Delta I = \Delta I_{max}\left(([L]+[P]+K_d)-\sqrt{([L]+[P]+K_d)^2-4[P][L]}\right)\Big/2[P],$$

where $[L]$ is the concentration of the peptide, $[P]$ is the concentration of the protein, ΔI is the observed change of signal intensity, and ΔI_{max} is the difference in signal intensity of the free and fully bound states of the protein. The K_d values were averaged over three separate experiments, with error calculated as the standard deviation between the runs.

Antibodies and peptides

The following antibodies were used for Western blotting with the indicated dilutions: anti-Flag M2 HRP (1:10000; Sigma), anti-HA HRP (1:1000; Roche), anti-HA.11 (1:1000; Babco), anti-HBO1 (1:2000; Abcam), anti-hEaf6 (1:1000; Abcam), anti-MORF (1:1000) (Ullah et al. 2008), anti-ING5 (1:1000; Abcam), and anti-H3 (1:5000; Abcam). For ChIP and ChIP-seq, the following antibodies were used: anti-H3K4me3 (Abcam), anti-H3 (Abcam), anti-H4ac (Millipore), anti-H3K14ac (Millipore), anti-H3K23ac (Millipore), anti-ING5 (Abcam), anti-HBO1 (Abcam), anti-ING2 (Epitomics), anti-MRG15, and anti-BRPF2 (Bethyl Laboratories). Biotinylated histone peptides were purchased from Millipore.

HAT assays

Native human chromatin and free histone were purified as previously described (Utley et al. 1996). HAT assays with 300 ng

of histone peptides (Millipore), 500 ng of core histones, or 500 ng of H1-depleted oligonucleosomes prepared from HeLa S3 cells were performed in a 15-μL reaction containing 50 mM Tris-HCl (pH 8.0), 10% glycerol, 1 mM DTT, 0.1 mM EDTA, 1 mM PMSF, 10 mM sodium butyrate (Sigma), and 1.25 nCi ^{3}H-labeled (Perkin Elmer Life Sciences) or unlabeled acetyl-CoA (Sigma). Samples were either spotted on P81 membranes (GE Healthcare) for counting or loaded on 18% SDS-PAGE gels. For gel assays, Coomassie staining was followed by EN^{3}HANCE (Perkin Elmer) treatment and fluorography.

ChIP assays

Chromatin preparation from RKO cells was done as previously described (Avvakumov et al. 2012). For immunoprecipitation of chromatin, we used 200 μg of chromatin with 1–3 μg of specific antibodies incubated overnight at 4°C. Next, 40 μL of Protein A Dynabeads (Invitrogen) was added to each sample and incubated for 4 h at 4°C. The beads were washed extensively and eluted with 1% SDS and 0.1 M $NaHCO_3$. Cross-linked samples were reversed by heating overnight at 65°C in the presence of 0.2 M NaCl. Samples were then treated with RNase A and proteinase K for 2 h, and DNA was recovered by phenol-chloroform and ethanol precipitation. Quantitative real-time PCR corrected for primer efficiencies in the linear range was performed using SYBR Green I (Roche) on a LightCycler 480 (Roche). The error bars represent standard errors based on two independent experiments. The primers used for quantitative PCR amplified the following genomic regions (build hg18): p21 TSS chr6, 36,754,421–36,754,542; p21 + 2 kb chr6, 36,756,871–36,756,972; and intergenic chr12, 65,815,182–65,815,318.

ChIP-seq analysis

ChIP and library preparation for sequencing were done as previously described (Avvakumov et al. 2012). Samples were sequenced by 50-base-pair (bp) single reads on either a Genome Analyzer platform (HBO1, BRPF1/2, and input) or a HiSeq 2000 platform (H3K4me3, H3, IgG, ING2, and ING5) (Illumina). Raw sequences were mapped using Bowtie (PubMed identification [PMID]: 19261174) on build hg18 of the human genome and deposited in the Gene Expression Omnibus (GEO) database under accession number GSE47190. HBO1 and input data were previously deposited under accession number GSE33221. Uniquely mapped sequences were kept for downstream analysis. The global profiles at TSSs presented in Supplemental Figure 3 were produced using the University of California at Santa Cruz genome browser gene definitions and the Python package HTseq. We extended the reads to 200 bp to be in line with our sonication protocol. In the case of multiple TSSs associated with the same gene, we selected the one with the highest number of H3K4me3 mapped reads within 5000 bp around the TSS. For gene expression level in RKO cells, we used publicly available data from an Affymetrix U133 plus 2.0 chip (PMID: 16300372). The binning of genes by their level of expression was performed by first sorting the log2 expression level and then subdividing genes in four equal categories (quartiles). The heat maps presented in Figure 3 were generated using a custom script in R (http://www.r-project.org). Briefly, we computed the profile for every ChIP-seq experiment for every gene, considering 5000 bp on both sides of the TSS. We took the profile around the TSS and binned it at every 50 bp. We then generated the heat maps using the binned values. For all of the heat maps, genes were sorted by function of their expression values in the RKO cell line, with the most expressed genes at the top of the heat map (PMID: 16300372).

Acknowledgments

We thank Céline Roques for experimental help during revisions, and Calcul Québec/Compute Canada for the use of their supercomputers. This research is supported by grants from the Canadian Institutes of Health Research (CIHR) (MOP-64289 to J.C., and MOP-97957 to X.J.Y.) and the National Institutes of Health (NIH) (GM096863 and GM101664 to T.G.K., and GM60489 to S.T.). M.-E.L. is supported by a Fonds de Recherche du Québec–Santé studentship, and J.C. is a Canada Research Chair.

References

Abmayr SM, Yao T, Parmely T, Workman JL. 1993. Preparation of nuclear and cytoplasmic extracts from mammalian cells. *Curr Protoc Mol Biol* **12:** 12.1.1–12.1.9.

Agalioti T, Chen G, Thanos D. 2002. Deciphering the transcriptional histone acetylation code for a human gene. *Cell* **111:** 381–392.

Agricola E, Verdone L, Di Mauro E, Caserta M. 2006. H4 acetylation does not replace H3 acetylation in chromatin remodelling and transcription activation of Adr1-dependent genes. *Mol Microbiol* **62:** 1433–1446.

Aikawa Y, Katsumoto T, Zhang P, Shima H, Shino M, Terui K, Ito E, Ohno H, Stanley ER, Singh H et al. 2010. PU.1-mediated upregulation of CSF1R is crucial for leukemia stem cell potential induced by MOZ-TIF2. *Nat Med* **16:** 580–585.

Ali M, Yan K, Lalonde ME, Degerny C, Rothbart SB, Strahl BD, Cote J, Yang XJ, Kutateladze TG. 2012. Tandem PHD fingers of MORF/MOZ acetyltransferases display selectivity for acetylated histone H3 and are required for the association with chromatin. *J Mol Biol* **424:** 328–338.

Avvakumov N, Cote J. 2007a. Functions of myst family histone acetyltransferases and their link to disease. *Subcell Biochem* **41:** 295–317.

Avvakumov N, Cote J. 2007b. The MYST family of histone acetyltransferases and their intimate links to cancer. *Oncogene* **26:** 5395–5407.

Avvakumov N, Lalonde ME, Saksouk N, Paquet E, Glass KC, Landry AJ, Doyon Y, Cayrou C, Robitaille GA, Richard DE, et al. 2012. Conserved molecular interactions within the HBO1 acetyltransferase complexes regulate cell proliferation. *Mol Cell Biol* **32:** 689–703.

Boudreault AA, Cronier D, Selleck W, Lacoste N, Utley RT, Allard S, Savard J, Lane WS, Tan S, Cote J. 2003. Yeast enhancer of polycomb defines global Esa1-dependent acetylation of chromatin. *Genes Dev* **17:** 1415–1428.

Carrozza MJ, Utley RT, Workman JL, Cote J. 2003. The diverse functions of histone acetyltransferase complexes. *Trends Genet* **19:** 321–329.

Champagne KS, Saksouk N, Pena PV, Johnson K, Ullah M, Yang XJ, Cote J, Kutateladze TG. 2008. The crystal structure of the ING5 PHD finger in complex with an H3K4me3 histone peptide. *Proteins* **72:** 1371–1376.

Chittuluru JR, Chaban Y, Monnet-Saksouk J, Carrozza MJ, Sapountzi V, Selleck W, Huang J, Utley RT, Cramet M, Allard S, et al. 2011. Structure and nucleosome interaction of the yeast NuA4 and piccolo-NuA4 histone acetyltransferase complexes. *Nat Struct Mol Biol* **18:** 1196–1203.

de Almeida SF, Carmo-Fonseca M. 2012. Design principles of interconnections between chromatin and pre-mRNA splicing. *Trends Biochem Sci* **37:** 248–253.

Doyon Y, Selleck W, Lane WS, Tan S, Cote J. 2004. Structural and functional conservation of the NuA4 histone acetyltransferase complex from yeast to humans. *Mol Cell Biol* **24:** 1884–1896.

Doyon Y, Cayrou C, Ullah M, Landry AJ, Cote V, Selleck W, Lane WS, Tan S, Yang XJ, Cote J. 2006. ING tumor suppressor proteins are critical regulators of chromatin acetylation required for genome expression and perpetuation. *Mol Cell* **21:** 51–64.

Draker R, Ng MK, Sarcinella E, Ignatchenko V, Kislinger T, Cheung P. 2012. A combination of H2A.Z and H4 acetylation recruits Brd2 to chromatin during transcriptional activation. *PLoS Genet* **8:** e1003047.

Filippakopoulos P, Picaud S, Mangos M, Keates T, Lambert JP, Barsyte-Lovejoy D, Felletar I, Volkmer R, Muller S, Pawson T, et al. 2012. Histone recognition and large-scale structural analysis of the human bromodomain family. *Cell* **149:** 214–231.

Foy RL, Song IY, Chitalia VC, Cohen HT, Saksouk N, Cayrou C, Vaziri C, Cote J, Panchenko MV. 2008. Role of Jade-1 in the histone acetyltransferase (HAT) HBO1 complex. *J Biol Chem* **283:** 28817–28826.

Hargreaves DC, Crabtree GR. 2011. ATP-dependent chromatin remodeling: Genetics, genomics and mechanisms. *Cell Res* **21:** 396–420.

Huang J, Tan S. 2013. Piccolo NuA4-catalyzed acetylation of nucleosomal histones: Critical roles of an Esa1 Tudor/chromo barrel loop and an Epl1 enhancer of polycomb A (EPcA) basic region. *Mol Cell Biol* **33:** 159–169.

Hung T, Binda O, Champagne KS, Kuo AJ, Johnson K, Chang HY, Simon MD, Kutateladze TG, Gozani O. 2009. ING4 mediates crosstalk between histone H3 K4 trimethylation and H3 acetylation to attenuate cellular transformation. *Mol Cell* **33:** 248–256.

Iizuka M, Matsui T, Takisawa H, Smith MM. 2006. Regulation of replication licensing by acetyltransferase Hbo1. *Mol Cell Biol* **26:** 1098–1108.

Iizuka M, Sarmento OF, Sekiya T, Scrable H, Allis CD, Smith MM. 2008. Hbo1 Links p53-dependent stress signaling to DNA replication licensing. *Mol Cell Biol* **28:** 140–153.

Kasten M, Szerlong H, Erdjument-Bromage H, Tempst P, Werner M, Cairns BR. 2004. Tandem bromodomains in the chromatin remodeler RSC recognize acetylated histone H3 Lys14. *EMBO J* **23:** 1348–1359.

Katsumoto T, Aikawa Y, Iwama A, Ueda S, Ichikawa H, Ochiya T, Kitabayashi I. 2006. MOZ is essential for maintenance of hematopoietic stem cells. *Genes Dev* **20:** 1321–1330.

Kueh AJ, Dixon MP, Voss AK, Thomas T. 2011. HBO1 is required for H3K14 acetylation and normal transcriptional activity during embryonic development. *Mol Cell Biol* **31:** 845–860.

Laue K, Daujat S, Crump JG, Plaster N, Roehl HH, Kimmel CB, Schneider R, Hammerschmidt M. 2008. The multidomain protein Brpf1 binds histones and is required for Hox gene expression and segmental identity. *Development* **135:** 1935–1946.

Liu L, Qin S, Zhang J, Ji P, Shi Y, Wu J. 2012. Solution structure of an atypical PHD finger in BRPF2 and its interaction with DNA. *J Struct Biol* **180:** 165–173.

Maltby VE, Martin BJ, Brind'Amour J, Chruscicki AT, McBurney KL, Schulze JM, Johnson IJ, Hills M, Hentrich T, Kobor MS, et al. 2012. Histone H3K4 demethylation is negatively regulated by histone H3 acetylation in *Saccharomyces cerevisiae*. *Proc Natl Acad Sci* **109:** 18505–18510.

Miller CT, Maves L, Kimmel CB. 2004. moz regulates Hox expression and pharyngeal segmental identity in zebrafish. *Development* **131:** 2443–2461.

Miotto B, Struhl K. 2010. HBO1 histone acetylase activity is essential for DNA replication licensing and inhibited by Geminin. *Mol Cell* **37:** 57–66.

Mishima Y, Miyagi S, Saraya A, Negishi M, Endoh M, Endo TA, Toyoda T, Shinga J, Katsumoto T, Chiba T, et al. 2011. The Hbo1-Brd1/Brpf2 complex is responsible for global acetylation of H3K14 and required for fetal liver erythropoiesis. *Blood* **118:** 2443–2453.

Musselman CA, Lalonde ME, Cote J, Kutateladze TG. 2012. Perceiving the epigenetic landscape through histone readers. *Nat Struct Mol Biol* **19:** 1218–1227.

Nakanishi S, Sanderson BW, Delventhal KM, Bradford WD, Staehling-Hampton K, Shilatifard A. 2008. A comprehensive library of histone mutants identifies nucleosomal residues required for H3K4 methylation. *Nat Struct Mol Biol* **15:** 881–888.

Pena PV, Davrazou F, Shi X, Walter KL, Verkhusha VV, Gozani O, Zhao R, Kutateladze TG. 2006. Molecular mechanism of histone H3K4me3 recognition by plant homeodomain of ING2. *Nature* **442:** 100–103.

Perez-Campo FM, Borrow J, Kouskoff V, Lacaud G. 2009. The histone acetyl transferase activity of monocytic leukemia zinc finger is critical for the proliferation of hematopoietic precursors. *Blood* **113:** 4866–4874.

Qin S, Jin L, Zhang J, Liu L, Ji P, Wu M, Wu J, Shi Y. 2011. Recognition of unmodified histone H3 by the first PHD finger of bromodomain-PHD finger protein 2 provides insights into the regulation of histone acetyltransferases monocytic leukemic zinc-finger protein (MOZ) and MOZ-related factor (MORF). *J Biol Chem* **286:** 36944–36955.

Qiu Y, Liu L, Zhao C, Han C, Li F, Zhang J, Wang Y, Li G, Mei Y, Wu M, et al. 2012. Combinatorial readout of unmodified H3R2 and acetylated H3K14 by the tandem PHD finger of MOZ reveals a regulatory mechanism for HOXA9 transcription. *Genes Dev* **26:** 1376–1391.

Saksouk N, Avvakumov N, Champagne KS, Hung T, Doyon Y, Cayrou C, Paquet E, Ullah M, Landry AJ, Cote V, et al. 2009. HBO1 HAT complexes target chromatin throughout gene coding regions via multiple PHD finger interactions with histone H3 tail. *Mol Cell* **33:** 257–265.

Sapountzi V, Cote J. 2011. MYST-family histone acetyltransferases: Beyond chromatin. *Cell Mol Life Sci* **68:** 1147–1156.

Selleck W, Fortin I, Sermwittayawong D, Cote J, Tan S. 2005. The *Saccharomyces cerevisiae* piccolo NuA4 histone acetyltransferase complex requires the enhancer of polycomb A domain and chromodomain to acetylate nucleosomes. *Mol Cell Biol* **25:** 5535–5542.

Shahbazian MD, Grunstein M. 2007. Functions of site-specific histone acetylation and deacetylation. *Annu Rev Biochem* **76:** 75–100.

Shi X, Hong T, Walter KL, Ewalt M, Michishita E, Hung T, Carney D, Pena P, Lan F, Kaadige MR, et al. 2006. ING2 PHD domain links histone H3 lysine 4 methylation to active gene repression. *Nature* **442:** 96–99.

Shilatifard A. 2006. Chromatin modifications by methylation and ubiquitination: Implications in the regulation of gene expression. *Annu Rev Biochem* **75:** 243–269.

Siino JS, Yau PM, Imai BS, Gatewood JM, Bradbury EM. 2003. Effect of DNA length and H4 acetylation on the thermal stability of reconstituted nucleosome particles. *Biochem Biophys Res Commun* **302:** 885–891.

Stankunas K, Berger J, Ruse C, Sinclair DA, Randazzo F, Brock HW. 1998. The enhancer of polycomb gene of *Drosophila* encodes a chromatin protein conserved in yeast and mammals. *Development* **125:** 4055–4066.

Thomas T, Corcoran LM, Gugasyan R, Dixon MP, Brodnicki T, Nutt SL, Metcalf D, Voss AK. 2006. Monocytic leukemia zinc finger protein is essential for the development of long-term reconstituting hematopoietic stem cells. *Genes Dev* **20:** 1175–1186.

Tsai WW, Wang Z, Yiu TT, Akdemir KC, Xia W, Winter S, Tsai CY, Shi X, Schwarzer D, Plunkett W, et al. 2010. TRIM24

links a non-canonical histone signature to breast cancer. *Nature* **468:** 927–932.

Tse C, Sera T, Wolffe AP, Hansen JC. 1998. Disruption of higher-order folding by core histone acetylation dramatically enhances transcription of nucleosomal arrays by RNA polymerase III. *Mol Cell Biol* **18:** 4629–4638.

Ullah M, Pelletier N, Xiao L, Zhao SP, Wang K, Degerny C, Tahmasebi S, Cayrou C, Doyon Y, Goh SL, et al. 2008. Molecular architecture of quartet MOZ/MORF histone acetyltransferase complexes. *Mol Cell Biol* **28:** 6828–6843.

Utley RT, Owen-Hughes TA, Juan LJ, Cote J, Adams CC, Workman JL. 1996. In vitro analysis of transcription factor binding to nucleosomes and nucleosome disruption/displacement. *Methods Enzymol* **274:** 276–291.

van Attikum H, Gasser SM. 2009. Crosstalk between histone modifications during the DNA damage response. *Trends Cell Biol* **19:** 207–217.

Vezzoli A, Bonadies N, Allen MD, Freund SM, Santiveri CM, Kvinlaug BT, Huntly BJ, Gottgens B, Bycroft M. 2010. Molecular basis of histone H3K36me3 recognition by the PWWP domain of Brpf1. *Nat Struct Mol Biol* **17:** 617–619.

Voss AK, Thomas T. 2009. MYST family histone acetyltransferases take center stage in stem cells and development. *Bioessays* **31:** 1050–1061.

Voss AK, Collin C, Dixon MP, Thomas T. 2009. Moz and retinoic acid coordinately regulate H3K9 acetylation, Hox gene expression, and segment identity. *Dev Cell* **17:** 674–686.

Wang X, Hayes JJ. 2008. Acetylation mimics within individual core histone tail domains indicate distinct roles in regulating the stability of higher-order chromatin structure. *Mol Cell Biol* **28:** 227–236.

Wang Z, Zang C, Cui K, Schones DE, Barski A, Peng W, Zhao K. 2009. Genome-wide mapping of HATs and HDACs reveals distinct functions in active and inactive genes. *Cell* **138:** 1019–1031.

Yang XJ, Ullah M. 2007. MOZ and MORF, two large MYSTic HATs in normal and cancer stem cells. *Oncogene* **26:** 5408–5419.